Int. J. Heat Mass Transfer. Vol. 32, No. 5, pp. 811–823, 1989
Printed in Great Britain

0017–9310/89 $3.00 + 0.00
Pergamon Press plc

The effect of buoyancy on downward and upward laminar-flow convection in the entrance region between inclined parallel plates

E. NAITO
Department of Mechanical Engineering, Shiga Prefectural Junior College, 1900 Hassaka-cho, Hikone-shi, Shiga 522, Japan

and

Y. NAGANO
Department of Mechanical Engineering, Nagoya Institute of Technology, Gokiso-cho, Showa-ku, Nagoya 466, Japan

(*Received* 8 *January* 1988 *and in final form* 16 *September* 1988)

Abstract—Numerical experiments are performed to investigate the effects of buoyancy on the hydrodynamic and thermal characteristics of downward-flow laminar convection in the entrance region between inclined parallel plates. Numerical solutions are given for three thermal conditions of parallel plates with uniform wall temperature or insulation. These results are discussed in conjunction with those of an upward-flow case. For use in practical applications, correlation equations are developed for the skin-friction coefficient and the local Nusselt number. The critical values of Ra/Re for the occurrence of flow reversal are also presented by the use of correlation equations for the skin-friction coefficient.

1. INTRODUCTION

TO RESOLVE essential problems related to the heat transfer augmentation of laminar-flow convection in the entrance region of a circular tube or channel requires detailed information not available from the classical boundary layer theory (for example, leading edge effect, secondary-flow effect and influence of buoyancy on heat transfer). Hence, in the previous study [1], numerical experiments were systematically carried out to investigate flow and heat transfer characteristics in the upward entry flow between inclined parallel plates. The numerical results of skin-friction coefficient and local Nusselt number were expressed by the correlation equations that describe quantitatively the buoyancy and inclination-angle effects. It became evident that the heat transfer deterioration observed at the upper wall in the horizontal parallel plates [2, 3] disappeared with increasing inclination angles. Also, it was found that the buoyancy affected the skin-friction coefficient and the local Nusselt number in nearly the same manner. Since the calculations were made for strictly two-dimensional flows in the Rayleigh number ranges below the onset of thermal instability [4–8], the flow reversal in a two-dimensional vertical upward flow at much higher Rayleigh numbers obtained by Aung and Worku [9, 10] was not found in the previous study [1]. On the other hand, flow reversal due to opposing free convection in the downward entry flow between vertical parallel plates was reported by Cebeci *et al.* [11]. However, the developing flow/thermal fields when one wall is heated cannot be fully understood from their results, because the information obtained is limited to the case where both walls are heated equally.

Hence, as in the previous study [1], the present numerical investigation focuses on the combined forced and free convection of laminar downward flow in the entrance region between inclined parallel plates with more general thermal conditions (i.e. lower wall heated and upper wall insulated, lower wall insulated and upper wall heated, and both walls heated equally). The present calculations reveal how the developing downward flow and heat transfer in the entrance region are affected by buoyancy in terms of the inclination angles. The results are discussed in conjunction with those of the upward-flow case. To be utilized as data bases for design technology in thermal engineering, correlation equations are developed for the skin-friction coefficient and local Nusselt number at arbitrary inclination angles, and Reynolds and Rayleigh numbers. Also, the effects of Prandtl numbers, and the critical value $(Ra/Re)_c$ for the occurrence of flow reversal, are discussed.

2. GOVERNING EQUATIONS AND NUMERICAL METHOD

Consider the heat transfer problem of two-dimensional laminar flow in the entrance region between

NOMENCLATURE

C_f	skin-friction coefficient
c_p	specific heat
g	gravitational acceleration
h	heat transfer coefficient
L	hydrodynamic entrance length
Nu	Nusselt number, $4s'h'/\lambda'$
Pe	Peclet number, $Pr\,Re$
Pr	Prandtl number, $c'_p\mu'/\lambda'$
p	pressure
q	heat flux
Ra	Rayleigh number, $8c'_p\rho'_0 g'\beta'(t'_w-t'_0)s'^3/(\lambda'\nu')$
Re	Reynolds number, $4s'u'_0/\nu'$
s	one-half the spacing between parallel plates
t	temperature
u, v	velocity components in the x- and y-directions
x, y	axial and transverse coordinates.

Greek symbols

β	coefficient of thermal expansion
θ	dimensionless temperature, $(t'_w-t')/(t'_w-t'_0)$
λ	thermal conductivity
ν	kinematic viscosity
ξ	dimensionless axial coordinate, $(0.8x)^{0.8}/\{1+(0.8x)^{0.8}\}$
ρ	density
ϕ	inclination angle
ψ	stream function
ω	vorticity.

Subscripts

0, 1	values at inlet or lower wall, upper wall
b	bulk mean temperature
c	value at centerline or critical value
h, t	values of flow and thermal fields
w	value at wall.

Superscripts

$'$	dimensional variable
*	values of isothermal flow and pure forced convection.

parallel plates with uniform wall temperature, set at an angle ϕ to the horizontal (that is, $\phi > 0$ for upward flow, $\phi < 0$ for downward flow). It is assumed that both the velocity and temperature profiles at the inlet are uniform. As in the previous study [1], the following three thermal conditions are studied: one wall (upper or lower) maintained at a constant temperature with the other wall insulated, then the reverse case; both walls maintained at a constant temperature. For the coordinate system and symbols of the physical model shown in Fig. 1, the dimensionless variables chosen are $x = x'/(2s')$, $y = y'/(2s')$, $u = u'/u'_0$, $v = v'/u'_0$, $p = 2(p' + \rho'_0 g' y' \cos\phi + \rho'_0 g' x' \sin\phi)/(\rho'_0 u'^2_0)$ and $\theta = (t'_w - t')/(t'_w - t'_0)$. The governing equations for two-dimensional steady laminar flow can be written in dimensionless forms with stream and vorticity functions as follows:

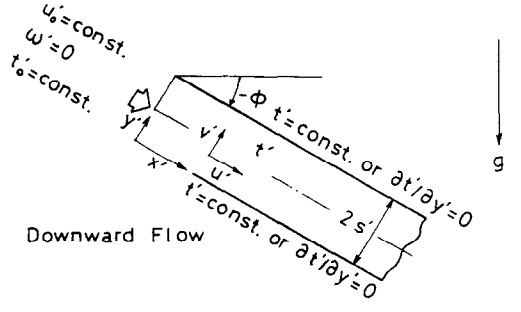

FIG. 1. Coordinate system.

$$\frac{d\xi}{dx}\left\{\frac{\partial}{\partial\xi}\left(\omega\frac{\partial\psi}{\partial y}\right)-\frac{\partial}{\partial y}\left(\omega\frac{\partial\psi}{\partial\xi}\right)\right\}=\frac{2}{Re}\nabla^2\omega + \frac{4Ra}{Pe\,Re}\left(\frac{\partial\theta}{\partial y}\sin\phi-\frac{d\xi}{dx}\frac{\partial\theta}{\partial\xi}\cos\phi\right) \quad (1)$$

$$\nabla^2\psi = \partial u/\partial y - \partial v/\partial x = -\omega \quad (2)$$

$$\frac{d\xi}{dx}\left\{\frac{\partial}{\partial\xi}\left(\theta\frac{\partial\psi}{\partial y}\right)-\frac{\partial}{\partial y}\left(\theta\frac{\partial\psi}{\partial\xi}\right)\right\}=\frac{2}{Pe}\nabla^2\theta \quad (3)$$

where the vorticity transport equation (1) is developed with the Boussinesq approximation so that only the density in the body-force term of the momentum equation is considered temperature dependent. Using the axial transformation, $\xi = (0.8x)^{0.8}/\{1+(0.8x)^{0.8}\}$, the region near the inlet is enlarged and the semi-infinite solution domain is converted into the finite one. The dimensionless stream function ψ and the Laplacian operator ∇^2 are defined as follows:

$$u = \partial\psi/\partial y, \quad v = -(d\xi/dx)\,\partial\psi/\partial\xi \quad (4)$$

$$\nabla^2 = (d\xi/dx)^2\,\partial^2/\partial\xi^2 + (d^2\xi/dx^2)\,\partial/\partial\xi + \partial^2/\partial y^2. \quad (5)$$

The boundary conditions for velocity and thermal fields are given as follows.

At $x = 0$ ($\xi = 0$) and $0 < y < 1$

$$u = 1, \quad \omega = 0, \quad \psi = y, \quad \theta = 1. \quad (6)$$

At $0 \leqslant x < \infty$ $(0 \leqslant \xi < 1)$ and $y = 0$ and 1

$$u = 0, \quad v = 0, \quad \psi_0 = 0, \quad \psi_1 = 1,$$

$$\partial\psi/\partial\xi = \partial\psi/\partial y = 0$$

$\theta = 0$ (at heated wall), $\partial\theta/\partial y = 0$ (at insulated wall). (7)

At $x \to \infty$ $(\xi = 1)$ and $0 \leqslant y \leqslant 1$

$$u = 6y(1-y), \quad v = 0, \quad \psi = 6y^2(1/2 - y/3)$$

$$\omega = -6(1-2y), \quad \theta = 0. \tag{8}$$

Note that the inlet conditions will affect the skin friction and heat transfer very near the inlet. However, practical difficulties arise from consideration of various conditions at the inlet in order to investigate the effects of buoyancy and inclination angle on various physical quantities. Since the effects of axial diffusion of momentum and heat on the upstream and/or downstream region of the inlet were investigated previously [12], we used the most usual inlet condition which is considered appropriate for this kind of study, as in the past.

Governing equations (1)–(3) are approximated by the set of finite difference equations using a central difference form, which are solved numerically by the SOR method. The discretization for the derivations of ψ and θ at the grid points adjacent to the lower and upper walls is performed in the same way as in the literature [2, 13]. The accuracy of the numerical solution is improved by separately deriving finite difference forms which satisfy the boundary conditions as closely as possible. For the vorticity at the wall, we adopted the finite difference form of three-order accuracy, which takes account of the buoyancy effect [1]. The mesh sizes $\Delta\xi = \Delta y = 0.02$, with each of the 51 grids in terms of ξ and y, are normally used. In order to increase the computing accuracy of heat transfer, the much smaller mesh size, $\Delta y = 0.005$, is used for $0 \leqslant y \leqslant 0.1$ and $0.9 \leqslant y \leqslant 1$ near the lower and upper walls, respectively. The iteration was continued until the convergence criteria, $|\psi_{i,j}^{k+1} - \psi_{i,j}^{k}|_{\max} < 10^{-6}$ and $|\theta_{i,j}^{k+1} - \theta_{i,j}^{k}|_{\max} < 10^{-6}$, were satisfied simultaneously, where k is the kth iteration of computations, and the subscript max is the maximum value of all mesh points of the network for each iteration.

3. RESULTS AND DISCUSSION

Computations were made with the basic parameters such as inclination angles, and Reynolds and Rayleigh numbers. The Reynolds number Re was varied from 50 to 300 in the same way as in the previous study [1], but the following discussion is mostly concerned with the results for $Re = 100$. The symbols A–I in the succeeding figures express velocity and temperature profiles at the typical axial locations given in Table 1.

Table 1. Locations where velocity and temperature profiles are given

	$x'/(2s')$
A	0.08019
B	0.22097
C	0.60892
D	1.25
E	1.87162
F	2.305
G	6.08134
H	19.4855
I	∞

3.1. *Velocity profile*

In order to determine the influence of the buoyancy on developing velocity profiles at various angles of inclination, Fig. 2 gives a comparison of velocity profiles at typical locations for $Re = 100$ and $Ra = 1500$. The results of a vertical upward-flow case have also been plotted in this figure. In downward flow, the fluid near the heated wall is decelerated by the opposite effect due to buoyancy. The flow rates are maintained constant so that the fluid near the opposite (insulated) wall is accelerated. Therefore, the velocity profile becomes fairly asymmetric. On the other hand, when both walls are heated equally, the fluid near the heated walls is decelerated, and the fluid in the core region is accelerated correspondingly. In addition, since the axial velocity u near the heated walls in the vertical upward flow is accelerated by free convection, the distortion of the velocity profile with inclination angle in downward flow has the tendency opposite to the result of upward flow.

Figure 3 gives a comparison of the difference in deceleration due to free convection at various Rayleigh numbers in the vertical downward flow. Because the location of the maximum cross-sectional velocity, when only one wall is heated, deviates from the centerline toward the insulated wall side with increasing Rayleigh number, then the velocity profile becomes appreciably asymmetric. At locations E and G for $Ra = 3000$, a flow reversal occurs at the heated wall by deceleration induced by free convection. In the case where both walls are heated, the flow reversal is not observed at $Ra = 3000$, but at $Ra = 5000$ the recirculation zone appears in the range $0.55 < x < 4$.

In Fig. 4, the development of centerline velocity u_c between vertical parallel plates with both walls heated equally is shown for both the downward and the upward flow cases at various Rayleigh numbers. With the development of the boundary layer, the u_c of the downward flow exhibits an overshoot beyond the value $u_c = 1.5$ of fully developed flow at some range of the entrance region. Although $(u_c)_{\max}$ values of overshoot become larger with increasing Rayleigh numbers, the location of $(u_c)_{\max}$ for the variations of Rayleigh numbers is around $x = 2.1$. On the other hand, when Ra becomes larger in the case with the upward flow, the deceleration of u_c appears tem-

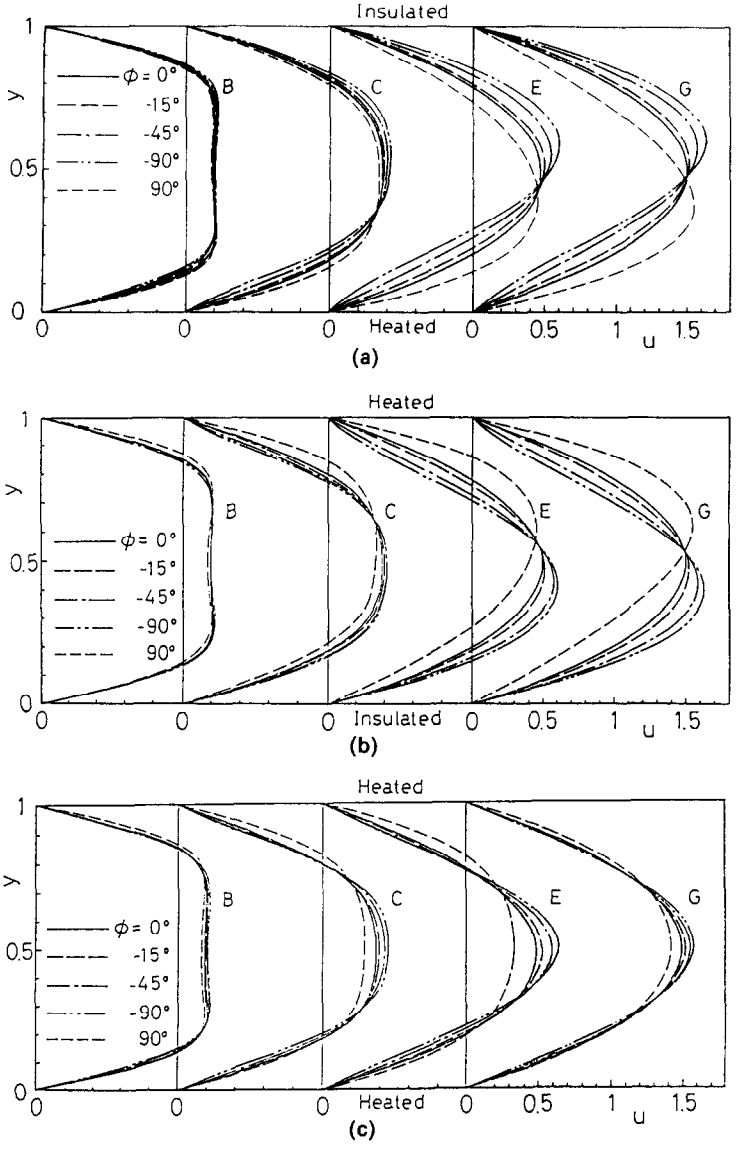

FIG. 2. Effects of inclination angles on developing velocity profiles for $Re = 100$, $Ra = 1500$ and $Pr = 0.71$: (a) lower wall heated; (b) upper wall heated; (c) both walls heated.

porarily in the entrance region. However, the centerline velocity is subsequently accelerated again, and u_c ultimately becomes 1.5.

3.2. *Temperature profile*

The distributions of isotherms and streamlines with flow reversal are shown in Fig. 5. Figure 5(a) reveals isotherms at $Re = 100$ and $Ra = 3000$ together with the results of both upward flow and pure forced convection in the absence of a buoyancy effect for comparison. It is known from this figure that fluid near the heated wall is decelerated in the downward flow so that the fluid temperature is quickly elevated. On the other hand, the temperature rise of fluid accelerated near the insulated wall is delayed. As seen from Fig. 5(b), the reversed flow appears in the recirculation zone having its center around $x \simeq 3.2$ and $y \simeq 0.88$ near the heated wall, and this recirculation zone extends over the range of $0.75 < x < 10$.

Figure 6 indicates how the developing temperature profiles between vertical parallel plates are changed by Rayleigh numbers. The corresponding velocity profiles have been shown in Fig. 3. Although the reversed flow appears at locations E and G for $Ra = 3000$ in the case with one wall heated, and at position E for $Ra = 5000$ in the case with both walls heated, the distortion of the temperature profile due to the flow reversal is not observed. Furthermore, in the downward flow the variation of temperature profiles with inclination angles (figure omitted) is found to be smaller than that of the velocity profiles in Fig. 2.

Figure 7 gives a comparison of the distributions of dimensionless bulk temperature, $(t'_b - t'_0)/(t'_w - t'_0)$, for

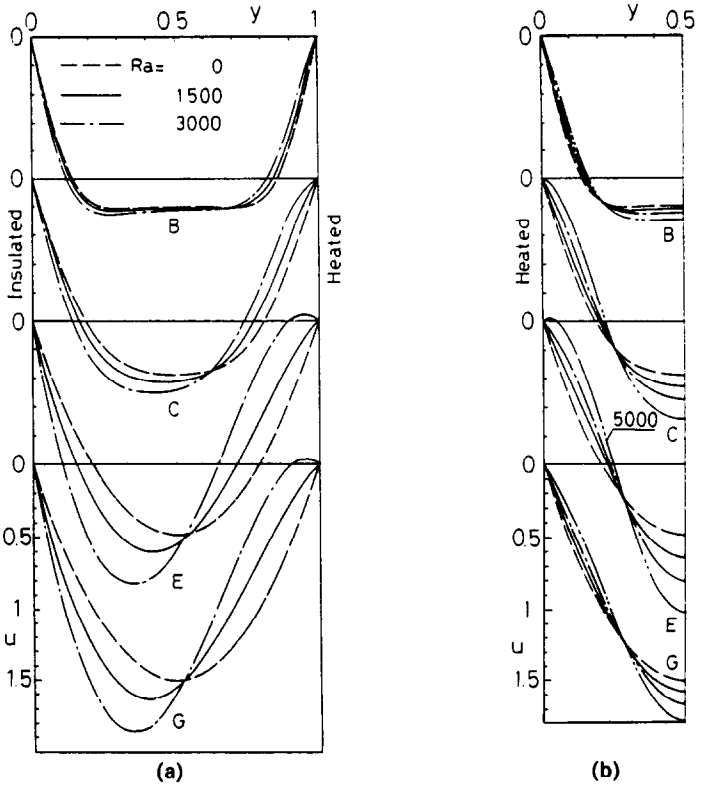

FIG. 3. Effects of Rayleigh numbers on developing velocity profiles in vertical channel for $Re = 100$ and $Pr = 0.71$: (a) one wall heated; (b) both walls heated.

vertical upward and downward flows. Here attention is paid to the location where the bulk temperature becomes $(t'_b - t'_0)/(t'_w - t'_0) = 1 - \theta_b = 0.5$. The location for the pure forced convection in the absence of a buoyancy effect is at around $x = 8.42$. As shown in Fig. 5, since the fluid temperature rise in the upward flow case becomes faster near the insulated wall, the location at $\theta_b = 0.5$ is $x = 7.35$ for $Ra = 1500$ and $x = 6.58$ for $Ra = 3000$, which is reduced by 13–20% in both cases. On the other hand, the location in the downward flow case is $x = 9.69$ for $Ra = 1500$ and $x = 11.2$ for $Ra = 3000$, which, conversely, is increased by 15–30%. In other words, the heat transfer of upward flow is more enhanced than in downward flow, and the same holds true in the case with both walls heated.

3.3. *Skin-friction coefficient and local Nusselt number*

The influence of buoyancy on the skin-friction coefficient and local Nusselt number changes with an

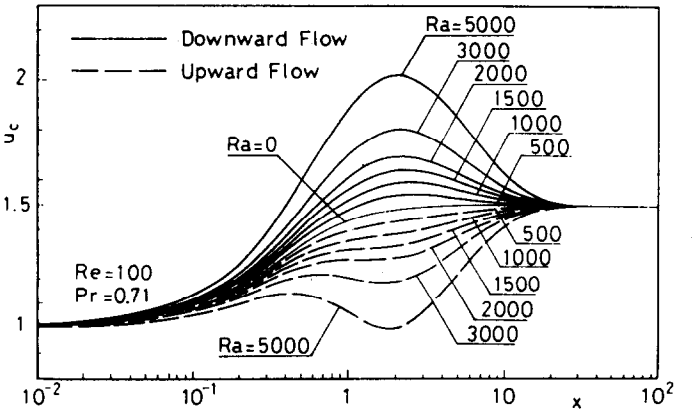

FIG. 4. Distributions of centerline velocity in downward and upward flow in a vertical channel with both walls heated.

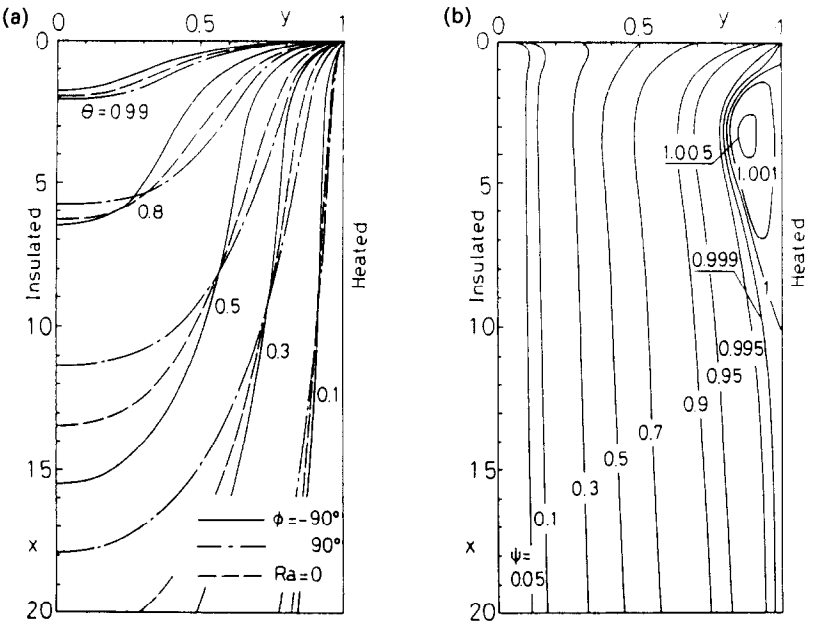

FIG. 5. Isotherms and streamlines in a vertical channel when only one wall is heated ($Re = 100$, $Ra = 3000$ and $Pr = 0.71$): (a) isotherms; (b) streamlines of downward flow.

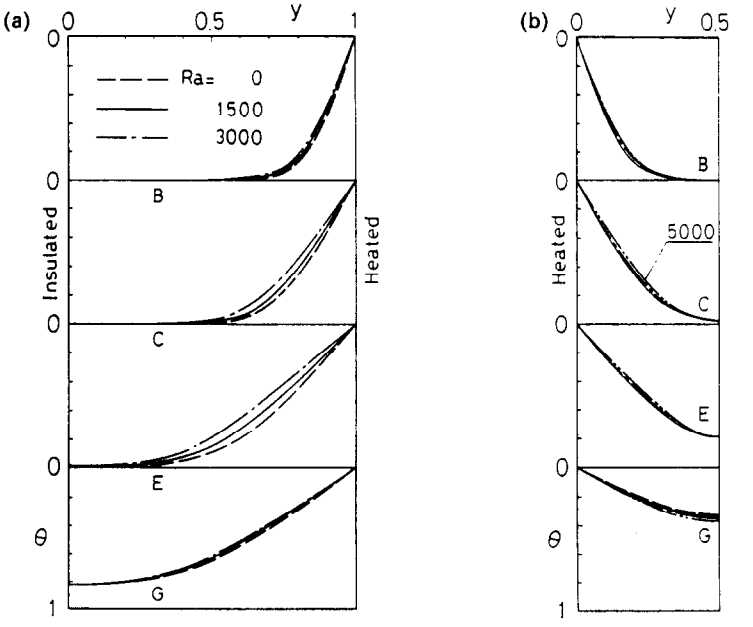

FIG. 6. Effects of Rayleigh numbers on developing temperature profiles in a vertical channel ($Re = 100$ and $Pr = 0.71$): (a) one wall heated; (b) both walls heated.

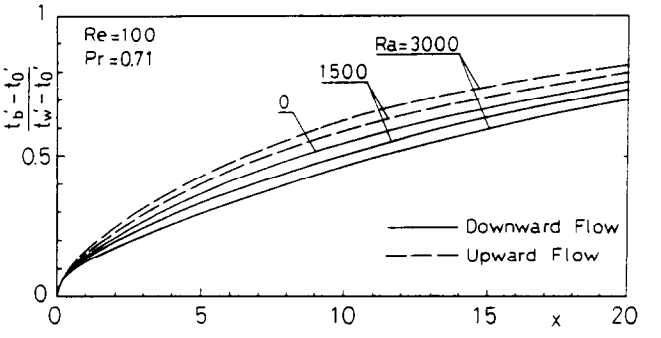

FIG. 7. Distributions of bulk temperature in a vertical channel when only one wall is heated.

inclination angle. When only one wall is heated, the C_f/C_f^* and Nu/Nu^* at various inclination angles for $Re = 100$ and $Ra = 1500$ are shown in Fig. 8 together with the results of upward flow for comparison. As shown by Fig. 8(a), the skin-friction coefficient at the lower wall (heated wall) in downward flow is decreased by the opposing flow component due to buoyancy and becomes lower with increasing distance from the inlet. Consequently, it reaches a minimum in the region $x = 0.3$–3. This is completely contrary to the result of upward flow where buoyancy assists the fluid motion. With the increase of inclination angles $-\phi$, the C_f/C_f^* values at both the heated wall and the insulated wall become smaller and larger, respectively, than C_f/C_f^* distributions at the horizontal channel. In the vertical channel, the location of $(C_f/C_f^*)_{min}$ in the downward flow and that of $(C_f/C_f^*)_{max}$ in the upward flow are both around $x = 3$.

As seen from Fig. 8(b), the local Nusselt numbers in the downward flow become lower than the result for the horizontal channel. This is because the thermal boundary layer in the downward flow grows much thicker due to the adverse effect of buoyancy with increasing inclination angles, which causes the temperature gradient at the heated wall to become smaller. The Nu/Nu^* variations reach a minimum at $x \simeq 2.3$ in a vertical downward flow and a maximum at $x \simeq 3.4$ in a vertical upward flow. These locations are in disagreement with those of minimum and maximum for C_f/C_f^*.

Next, in order to examine the influence of Rayleigh number variations on the skin-friction coefficient C_f and local Nusselt number Nu for the combined forced and free convection (downward flow and upward flow) between the vertical parallel plates with only one wall heated, the values of C_f and Nu for Rayleigh numbers ranging from 0 to 3000 at $Re = 100$ are shown in Fig. 9. It is seen that at $Ra = 3000$ the skin friction of downward flow becomes negative in the region $x = 0.7$–10, and the flow reversal develops in

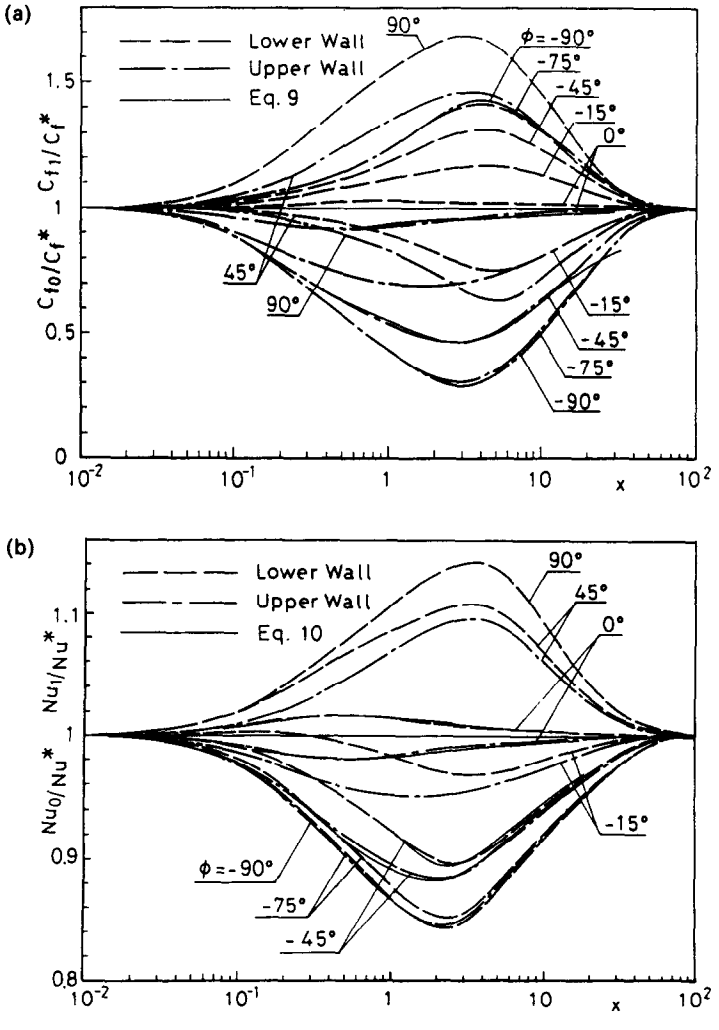

FIG. 8. Skin-friction coefficient and local Nusselt number affected by buoyancy at various inclination angles ($Re = 100$ and $Ra = 1500$): (a) skin-friction coefficient when only lower wall is heated; (b) local Nusselt number when either lower or upper wall is heated.

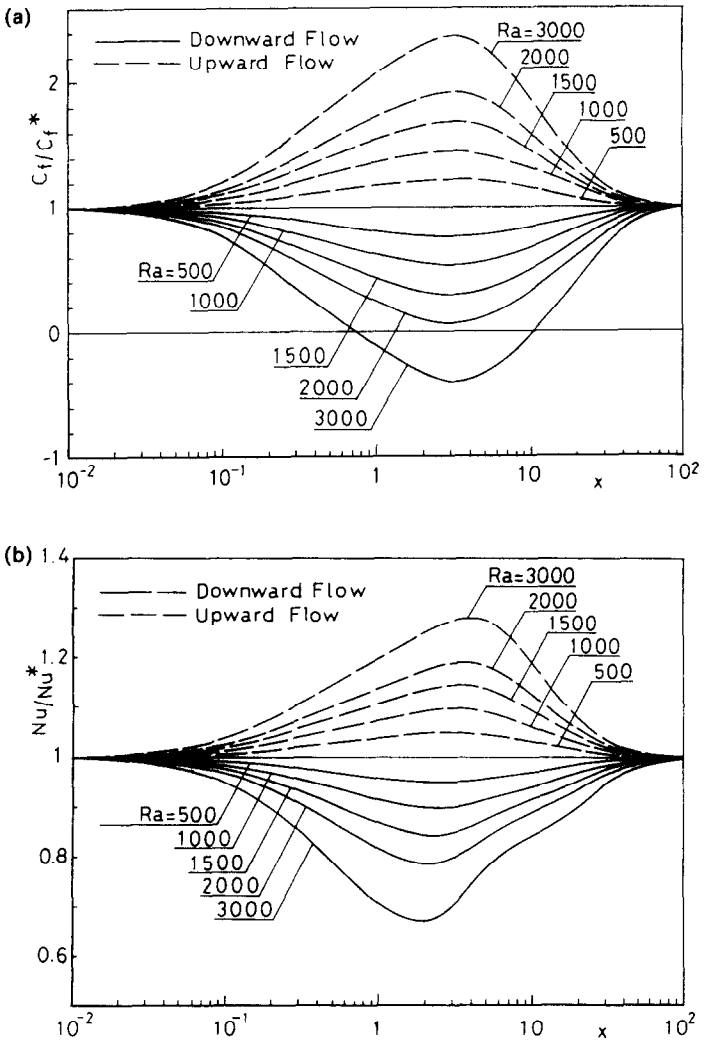

FIG. 9. Effects of Rayleigh number on skin-friction coefficient and local Nusselt number in a vertical channel with one wall heated ($Re = 100$ and $Pr = 0.71$): (a) skin-friction coefficient at the heated wall; (b) local Nusselt number.

this region. Although the corresponding Nu/Nu^* values become smaller, this effect is not so extreme because C_f/C_f^* brings about the change of sign.

The locations of both the maximum and minimum C_f/C_f^* are at $x \simeq 3$, and these locations are almost never affected by Rayleigh number variations. However, the positions where Nu/Nu^* becomes a maximum (upward flow) or a minimum (downward flow) moves slightly downstream in an upward flow case or upstream in a downward flow case with increasing Rayleigh number. Although there is a similarity between the distributions of $|1-C_f/C_f^*|/|1-C_f/C_f^*|_{max}$ and $|1-Nu/Nu^*|/|1-Nu/Nu^*|_{max}$ in the upward flow case [1], this tendency cannot be found in downward flow. Therefore, the correlation equations for the downward flow will show more appreciable complexity than for the upward flow case. However, because correlation equations are useful from the practical standpoint of design technology, those for the skin-friction coefficient and local Nusselt number are obtained as follows.

(1) When only one wall is heated:

$$C_f = C_f^*\{1+A(F+B\cdot f)\} \tag{9}$$

where

$$F = 4\zeta(1-\zeta),$$

$$Nu = Nu^*\{1+A(F+B\cdot f)\}, \quad 0 \leqslant \zeta \leqslant 1 \tag{10}$$

where

$$F = \zeta(3.124+13.81\zeta-106.1\zeta^2+246\zeta^3 - 196.3\zeta^4), \quad 0 \leqslant \zeta \leqslant 0.5$$

$$= 1+(\zeta-0.5)\{0.4093-18.02(\zeta-0.5) +78.71(\zeta-0.5)^2-168.4(\zeta-0.5)^3 +123.5(\zeta-0.5)^4\}, \quad 0.5 \leqslant \zeta \leqslant 1.$$

(2) When both walls are heated equally:

$$C_f = C_f^*\{1+A(F+B\cdot f)\} \tag{11}$$

where

$$F = 4\zeta(1-\zeta), \quad 0 \leqslant \zeta \leqslant 0.5$$
$$= 1+(\zeta-0.5)\{0.08154-9.323(\zeta-0.5)+32.91(\zeta-0.5)^2-133.1(\zeta-0.5)^3+179.4(\zeta-0.5)^4\}, \quad 0.5 \leqslant \zeta \leqslant 1$$

$$Nu_0 = Nu^*[1+\{(0.008FRa\sin\phi)/Re-A(F+B\cdot f)\}] \tag{12}$$

$$Nu_1 = Nu^*\{1+A(F+B\cdot f)\} \tag{13}$$

where

$$F = \zeta(1.271+25.23\zeta-118.9\zeta^2+214.5\zeta^3-143.7\zeta^4), \quad 0 \leqslant \zeta \leqslant 0.5$$
$$= 1+(\zeta-0.5)\{0.3786-14.83(\zeta-0.5)+72.44(\zeta-0.5)^2-209.6(\zeta-0.5)^3+208.6(\zeta-0.5)^4\}, \quad 0.5 \leqslant \zeta \leqslant 1.$$

Here factors A, B and f of equations (9)–(13) are given as follows:

$$A = (a_0+a_1\sin\phi+a_2\sin^2\phi+a_3\sin^3\phi+a_4\sin^4\phi+a_5\sin^5\phi)Ra/Re$$
$$B = b_0+b_1\chi+b_2\chi^2+b_3\chi^3+b_4\chi^4+b_5\chi^5)$$
$$f = c_1\zeta+c_2\zeta^2+c_3\zeta^3+c_4\zeta^4+c_5\zeta^5, \quad 0 \leqslant \zeta \leqslant P$$
$$= d_1(0.5-\zeta)+d_2(0.5-\zeta)^2+d_3(0.5-\zeta)^3+d_4(0.5-\zeta)^4+d_5(0.5-\zeta)^5, \quad P \leqslant \zeta \leqslant 0.5$$
$$= 0, \quad 0.5 \leqslant \zeta \leqslant 1$$

where $\chi = 1+\sin\phi$, $\zeta = X/(1+X)$ and $X = x/(x_h)_{\min}$ or $x/(x_t)_{\min}$. The values of coefficients ($a_0, a_1, a_2, \ldots$, $b_0, b_1, b_2, \ldots$, $c_0, c_1, c_2, \ldots$ and $d_0, d_1, d_2, \ldots$) and the applicable ranges of these equations are shown in Table 2. Furthermore, at the lower wall, except for the case with the upper wall maintained at a constant temperature, the sign of B is reversed when the value of A becomes positive.

The locations where C_f/C_f^* and Nu/Nu^* become minimum are given, respectively, as follows:

$$(x_h)_{\min} = C\,Re^n \tag{14}$$

$$(x_t)_{\min} = C\,Re^n. \tag{15}$$

In the above set, the calculated values at $\phi = -90°$ and $Ra = 1500$ (for the lower wall) and at $\phi = -75°$ and $Ra = 1500$ (for the upper wall) are assigned to the $(x_h)_{\min}$ and $(x_t)_{\min}$ values.

As an example, the values predicted from the correlation equations are included in Fig. 8 for $\phi = 0°$ and $-45°$. When only one wall is heated with $\phi = -45°$, the errors for predictions of C_f are 2.5% at the most; those for Nu are 1%. Thus, if the C_f^* and Nu^* for $Ra = 0$ are known, the C_f and Nu at arbitrary Reynolds and Rayleigh numbers, and inclination angle are obtained from the present correlation equations. The applicable range of these correlation equations is $0.05 \leqslant x \leqslant 10$ for $0 \leqslant Ra \leqslant 5000$, $50 \leqslant Re \leqslant 300$ and $Pr = 0.71$.

3.4. *Critical value for flow reversal*

The prediction of the critical Rayleigh number for the case of flow reversal ($C_f \leqslant 0$) is very important in the design of engineering devices. Thereupon, $(Ra/Re)_c$ for inclination angles can be calculated easily by applying the correlation equations of skin-friction coefficient in Section 3.3. The calculated results are shown in Fig. 10. It is seen in this figure that the critical Ra/Re when only one wall is heated becomes lower than when both walls are heated equally. In addition, with either one wall or both walls heated, $(Ra/Re)_c$ at the upper wall becomes lower than at the lower wall.

3.5. *Buoyancy and Prandtl number*

The influence of buoyancy on the air ($Pr = 0.71$) flow has been investigated above from the standpoint of thermal design technology. If the fluid varies, Prandtl number varies as well. Also, the thermal field depends generally on the Prandtl number. Therefore, the Prandtl number effect at $Ra = 1500$ and $Re = 100$ is demonstrated here. To give a typical example of the effect which the buoyancy exerts on the upward and downward flow between vertical parallel plates, the results at $Pr = 0.07$, 0.71 and 7 are discussed in a basic fashion. The differences in the developing velocity profiles at the three Prandtl numbers are shown in Fig. 11. In the downward flow of $Pr = 0.07$, the reversed flow occurs in the region near the inlet wall, and the fluid in the core region is accelerated considerably. In the upward-flow case, since the fluid near the heated wall is accelerated by the additive effect due to buoyancy, the fluid in the core region is decelerated below the initial velocity. As a result, the velocity

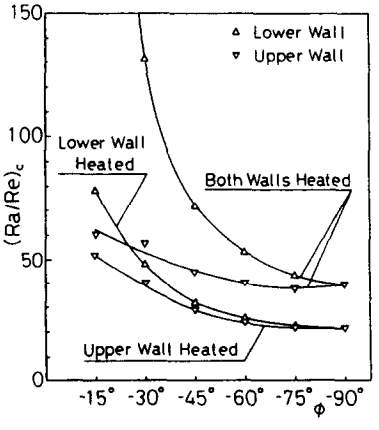

FIG. 10. Critical values for flow reversal (with $Pr = 0.71$).

Table 2. Coefficients in polynomial expansions A, B and f

		C_f				Nu		
		One wall heated		Both walls heated		One wall heated		Both walls heated
		At LW (LWH)	At UW (UWH)	At LW	At UW	At LW (LWH)	At UW (UWH)	At LW and UW
A	a_0	0.02508	−0.003234	0.00536	−0.005808	0.000603	−0.00067	−0.001568
	a_1	0.1507	0.1985	0.05318	0.1617	0.00936	0.00195	0.001849
	a_2	0.6436	0.9471	0.2113	0.8276	−0.002922	−0.06409	−0.0213
	a_3	1.447	2.101	0.5621	1.821	0.00166	−0.1715	−0.06669
	a_4	1.402	1.999	0.6206	1.739	0.009688	−0.1892	−0.08248
	a_5	0.4965	0.6917	0.2472	0.6063	0.006797	−0.07404	−0.03641
B	b_0	$0.0028\sqrt{(Ra)}$	$0.0028\sqrt{(Ra)}$	0.098	0.098	0	0	$0.6(0.01-1/Ra)$
	b_1	−0.8547	0.009	−1.097	−0.1162	−1.24	0.9839	−0.07285
	b_2	4.222	−2.62	3.972	3.938	1.006×10^1	−5.443	0.85
	b_3	-1.385×10^1	7.855	−9.658	-1.331×10^1	4.059×10^1	1.692×10^1	1.426
	b_4	-1.213×10^1	6.653	5.941	1.708×10^1	6.513×10^1	-2.387×10^1	−0.8513
	b_5	2.061×10^1	-1.126×10^1	0	7.097	-3.469×10^1	1.271×10^1	0
	C	0.059	0.0523	0.027	0.0243	0.042	0.0378	0.0162
	n	0.87	0.87	0.9	0.9	0.87	0.87	0.9
Range		$0°\geqslant\phi\geqslant-90°$	$0°\geqslant\phi>-90°$	$0°\geqslant\phi\geqslant-90°$	$0°\geqslant\phi>-90°$	$0°\geqslant\phi\geqslant-90°$	$0°\geqslant\phi>-90°$	$0°\geqslant\phi\geqslant-90°$
f	c_1	-1.639×10^1		-3.139×10^1		6.189	1.69	−2.96
	c_2	1.616×10^3		1.134×10^3		2.347×10^2	1.895	2.975×10^2
	c_3	-3.171×10^4		-1.256×10^4		-3.752×10^3	-1.538×10^3	3.381×10^3
	c_4	2.651×10^5		6.261×10^4		2.093×10^4	1.676×10^3	-1.578×10^4
	c_5	-8.31×10^5		-1.2×10^5		-4.142×10^4	1.045×10^4	2.662×10^4
f	d_1	0.3518		−1.773		−3.845	−6.939	−4.692
	d_2	1.149×10^1		-3.734×10^1		9.914	-6.983×10^1	3.772×10^1
	d_3	6.768×10^1		-3.977×10^2		8.369×10^1	-5.52×10^2	4.359×10^2
	d_4	3.415×10^2		-1.192×10^3		2.194×10^2	-1.825×10^3	1.618×10^3
	d_5	4.982×10^2		-1.107×10^3		2.409×10^2	-2.067×10^3	2.117×10^3
	P	0.106		0.167		0.175	0.156	0.217

LWH, lower wall heated; UWH, upper wall heated; LW, lower wall; UW, upper wall.

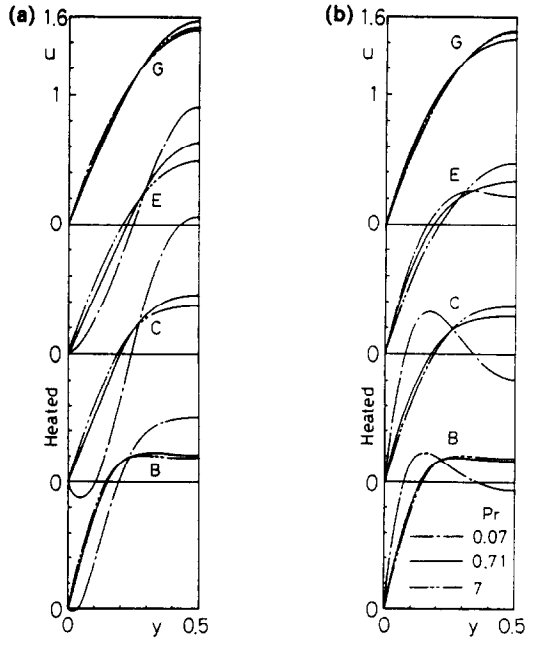

FIG. 11. Effects of Prandtl number on developing velocity profiles in vertical channel with both walls heated ($Re = 100$ and $Ra = 1500$): (a) downward flow; (b) upward flow.

profile becomes very concave at locations B and C. At $Pr = 7$, the developing velocity profiles of the isothermal flow do not differ enough to be drawn separately from that of the downward flow or the upward flow.

The effects of Pr on C_f and Nu are demonstrated in Fig. 12. The locations for $(C_f/C_f^*)_{max}$ and $(C_f/C_f^*)_{min}$ are around $x = 1.5$ at $Pr = 0.71$, $x = 0.4$–0.6 at $Pr = 0.07$ and $x \simeq 6$ at $Pr = 7$. On the other hand, the maximum and minimum for Nu/Nu^* are around $x = 1.1$ at $Pr = 0.71$, against $x \simeq 0.6$ at $Pr = 0.07$ and $x \simeq 3$ at $Pr = 7$. In other words, the effects which the buoyancy exerts on the distributions of the skin-friction coefficient and local Nusselt number are strongly dependent on Prandtl number.

In concluding this section, a cautionary note must be added. In a heat transfer problem with a large q'_w or a large temperature difference $(t'_w - t'_0)$, an analysis taking account of fluid property variation is necessary. As reported by Suzuki *et al.* [14] and Kieda *et al.* [15], the local Nusselt number in a vertical tube is affected by the variation of fluid properties, flow direction (upward or downward), the Prandtl and Reynolds numbers, and the heating conditions (e.g. q'_w = const. or t'_w = const.). It is difficult to find a general cor-

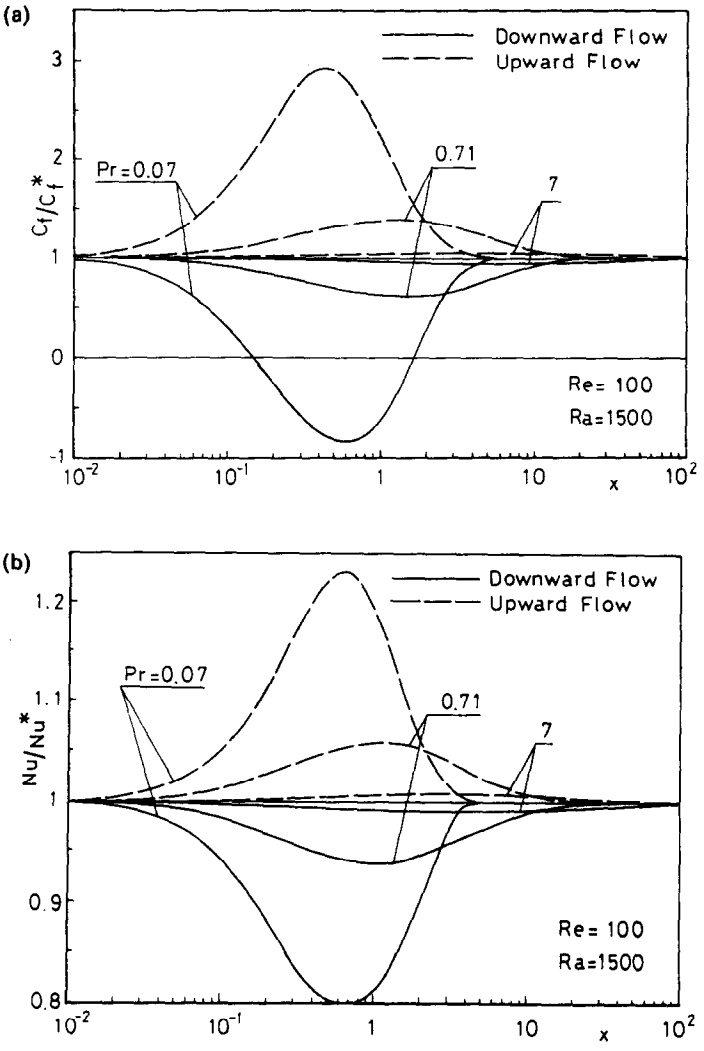

FIG. 12. Effects of Prandtl number on skin-friction coefficient and local Nusselt number in a vertical channel with both walls heated ($Re = 100$ and $Ra = 1500$): (a) skin-friction coefficient; (b) local Nusselt number.

relation equation for the local Nusselt number. Hence, Kieda *et al.* [15] proposed to make use of numerical computation as often as the heat transfer problem in this regime occurs. From the standpoint of thermal design technology, however, an accumulation of data bases on heat transfer engineering is now required. So, in this study, we dealt with only two-dimensional problems below the onset of thermal instability and obtained correlation equations with superposed buoyancy effect on the skin-friction coefficient C_f^* and local Nusselt number Nu^* in pure forced convection. Accordingly, we must leave the problems of property variation and secondary flow for future study.

4. CONCLUSIONS

A numerical investigation has been made of combined forced and free convection of downward flow in the entrance region between inclined parallel plates with uniform wall temperature. We can draw the following conclusions.

(1) The velocity profiles in the entrance region are distorted by buoyancy, the effect of which is dependent upon the inclination angles. The fluid near the heated wall is decelerated by opposing flow components induced by buoyancy. As a result, since the flow rate is maintained constant, the fluid near the opposite (insulated) wall is accelerated when only one wall is heated, and the fluid in the core region is accelerated when both walls are heated equally.

(2) The variation of temperature profiles with inclination angle is found to be smaller than that of the corresponding velocity profiles.

(3) With increasing inclination angles, the skin-friction coefficients become smaller at the heated wall and greater at the insulated wall than those of a horizontal channel.

(4) The values of local Nusselt number, on the other hand, become consistently smaller than those of a horizontal channel with increasing inclination angles.

(5) The correlation equations for the values of local Nusselt number and skin-friction coefficient at the heated wall are developed for use in practical applications.

(6) The critical values of Ra/Re for the flow reversal occurring at the heated wall are predicted from the correlation equations for the skin-friction coefficient.

(7) The influence of buoyancy becomes greater with decreasing Prandtl numbers.

REFERENCES

1. E. Naito and Y. Nagano, Combined forced and free upward-flow convection in the entrance région between inclined parallel plates, *Trans. ASME*, Series C, *J. Heat Transfer* (1989), to be published.
2. E. Naito, Buoyancy force effects on laminar flow and heat transfer in the entrance region between horizontal parallel plates, *Heat Transfer—Jap. Res.* **13,** 80–96 (1984).
3. E. Naito, The effect of buoyancy on laminar flow and heat transfer in the entrance region between horizontal parallel plates, *Int. Chem. Engng* **25,** 315–323 (1985).
4. Y. Mori and Y. Uchida, Forced convective heat transfer between horizontal flat plates, *Int. J. Heat Mass Transfer* **9,** 803–817 (1966).
5. W. Nakayama, G. J. Hwang and K. C. Cheng, Thermal instability in plane Poiseuille flow, *Trans. ASME*, Series C, *J. Heat Transfer* **92,** 61–68 (1970).
6. G. J. Hwang and K. C. Cheng, Convective instability in the thermal entrance region of a horizontal parallel plate channel heated from below, *Trans. ASME*, Series C, *J. Heat Transfer* **95,** 72–77 (1973).
7. K. C. Cheng and R.-S. Wu, Axial heat conduction effects on thermal instability of horizontal plane Poiseuille flows heated from below, *Trans. ASME*, Series C, *J. Heat Transfer* **98,** 564–569 (1976).
8. K. Fukui, M. Nakajima, H. Ueda and T. Mizushina, Flow instability and transport phenomena in combined free and forced convection between vertical parallel plates, *J. Chem. Engng Japan* **15,** 172–180 (1982).
9. W. Aung and G. Worku, Developing flow and flow reversal in a vertical channel with asymmetric wall temperature, *Trans. ASME*, Series C, *J. Heat Transfer* **108,** 299–304 (1986).
10. W. Aung and G. Worku, Theory of fully developed, combined convection including flow reversal, *Trans. ASME*, Series C, *J. Heat Transfer* **108,** 485–488 (1986).
11. T. Cebeci, A. A. Khattab and R. LaMont, Combined natural and forced convection in vertical ducts, *Proc. 7th Int. Heat Transfer Conf.*, Vol. 2, pp. 419–424 (1982).
12. E. Naito, Fluid flow and heat transfer near the leading edge of parallel plates, *Proc. ASME–JSME Thermal Engng Joint Conf.*, Vol. 3, pp. 35–41 (1983).
13. E. Naito, Laminar forced convection heat transfer in the air flow through a cascade of parallel plates: the case of uniform heat flux. In *Heat Transfer Science and Technology* (Edited by Bu-Xuan Wang), pp. 228–236. Hemisphere, Washington, DC (1987).
14. K. Suzuki, S. Kieda, T. Chichiki and T. Sato, Numerical study of convective heat transfer with variable fluid properties in the inlet region of a circular tube. In *Numerical Methods in Thermal Problems* (Edited by R. W. Lewis and K. Morgan), Pinneridge Press, Swansea (1981).
15. S. Kieda, T. Chichiki, K. Shimaoka, K. Suzuki and T. Sato, Forced–natural combined heat transfer in the inlet region of a vertical pipe, *Trans. Jap. JSME*, Series B **48–430,** 1111–1119 (1982).

EFFET DU FLOTTEMENT SUR LA CONVECTION LAMINAIRE DESCENDANTE ET ASCENDANTE DANS LA REGION D'ENTREE ENTRE DES PLANS PARALLELES INCLINES

Résumé—Des expériences numériques sont conduites pour étudier les effets du flottement sur les caractéristiques hydrodynamiques et thermiques de la convection laminaire descendante dans la région d'entrée entre plans parallèles inclinés. Des solutions numériques sont données pour trois conditions thermiques avec température pariétale uniforme ou isolation sur les plans. Ces résultats sont discutés en liaison avec ceux du cas de l'écoulement ascendant. Pour l'utilisation dans des cas pratiques, des formules sont développées en ce qui concerne le coefficient de frottement et le nombre de Nusselt. Les valeurs critiques de Ra/Re dans le cas de l'écoulement de retour sont aussi présentées par des formules pour le coefficient de frottement.

EINFLUSS DES AUFTRIEBS AUF DIE LAMINARE AUFWÄRTS- UND ABWÄRTSSTRÖMUNG IM EINLAUFBEREICH ZWISCHEN ZWEI GENEIGTEN PARALLELEN PLATTEN

Zusammenfassung—Der Einfluß des Auftriebs auf das thermische und hydrodynamische Verhalten einer nach unten gerichteten laminaren Konvektionsströmung im Einlaufbereich zweier geneigter paralleler Platten wurde numerisch untersucht. Lösungen für drei thermische Randbedingungen an den Platten (homogene Oberflächentemperatur bzw. ideale Wärmedämmung) werden vorgestellt. Die Ergebnisse werden mit denjenigen für eine aufsteigende laminare Strömung verglichen und diskutiert. Für die praktische Anwendung werden Korrelationen für den Wandreibungskoeffizienten und die örtliche Nusselt-Zahl bestimmt. Die kritischen Werte von Ra/Re, welche die Strömungsumkehr charakterisieren, werden mit Hilfe der Korrelation für den Wandreibungskoeffizienten angegeben.

ВЛИЯНИЕ ПОДЪЕМНЫХ СИЛ НА НИСХОДЯЩИЙ И ВОСХОДЯЩИЙ ЛАМИНАРНЫЕ КОНВЕКТИВНЫЕ ПОТОКИ НА НАЧАЛЬНОМ УЧАСТКЕ ЗАЗОРА МЕЖДУ НАКЛОННЫМИ ПАРАЛЛЕЛЬНЫМИ ПЛАСТИНАМИ

Аннотация—Проведены численные эксперименты для исследования влияния подъемных сил на гидродинамические и тепловые характеристики нисходящего ламинарного течения на начальном участке канала, образованного наклонными параллельными пластинами. Численные решения представлены для трех видов тепловых условий на пластинах, которые либо однородно нагреты, либо теплоизолированы. Полученные результаты рассматриваются совместно с соответствующими данными для случая восходящего течения. В целях практических приложений выводятся критериальные зависимости для гидравлического коэффициента трения и локального числа Нуссельта. С помощью критериальных зависимостей для коэффициента трения получены критические значения Ra/Re, при которых возникает возвратное течение.